⊕ISME

Ecological drivers switch from bottom–up to top–down during model microbial community successions

Sven P. Tobias-Hünefeldt (ID)[1,2] · Jess Wenley (ID)[1,2] · Federico Baltar (ID)[3] · Sergio E. Morales (ID)[1]

Abstract

Bottom–up selection has an important role in microbial community assembly but is unable to account for all observed variance. Other processes like top–down selection (e.g., predation) may be partially responsible for the unexplained variance. However, top–down processes and their interaction with bottom–up selective pressures often remain unexplored. We utilised an in situ marine biofilm model system to test the effects of bottom–up (i.e., substrate properties) and top–down (i.e., large predator exclusion via 100 μm mesh) selective pressures on community assembly over time (56 days). Prokaryotic and eukaryotic community compositions were monitored using 16 S and 18 S rRNA gene amplicon sequencing. Higher compositional variance was explained by growth substrate in early successional stages, but as biofilms mature, top–down predation becomes progressively more important. Wooden substrates promoted heterotrophic growth, whereas inert substrates' (i.e., plastic, glass, tile) lack of degradable material selected for autotrophs. Early wood communities contained more mixotrophs and heterotrophs (e.g., the total abundance of Proteobacteria and Euglenozoa was 34% and 41% greater within wood compared to inert substrates). Inert substrates instead showed twice the autotrophic abundance (e.g., cyanobacteria and ochrophyta made up 37% and 10% more of the total abundance within inert substrates than in wood). Late native (non-enclosed) communities were mostly dominated by autotrophs across all substrates, whereas high heterotrophic abundance characterised enclosed communities. Late communities were primarily under top–down control, where large predators successively pruned heterotrophs. Integrating a top–down control increased explainable variance by 7–52%, leading to increased understanding of the underlying ecological processes guiding multitrophic community assembly and successional dynamics.

Introduction

Microbiome compositions across many ecosystems have been extensively studied, but mechanistic understanding of successions leading to their formation remains poor,

✉ Sergio E. Morales
   sergio.morales@otago.ac.nz

[1] Department of Microbiology and Immunology, University of Otago, PO Box 56, Dunedin 9054, New Zealand

[2] Department of Marine Science, University of Otago, PO Box 56, Dunedin 9054, New Zealand

[3] Department of Functional & Evolutionary Ecology, Division of Bio-Oceanography, University of Vienna, Althanstrasse 14, A-1090 Vienna, Austria

especially the relative importance of bottom–up and top–down controls. Historic pure culture approaches, which remove biotic interactions, have led to a focus on resource limitations as a mechanism to explain differences in growth and community composition [1, 2]. However, biotic interactions have the potential to impact microbiome assembly and composition [3]. Microbiome studies generally report 20–67% [4–6] unexplained composition variance when utilising resource limitations as an explanatory variable. Unexplained variance represents a fundamental knowledge gap within the microbial ecology field and suggests that other processes must be contributing to microbiome changes.

Previous studies have found that communities can be shaped by two possible overarching processes: stochastic and deterministic. Stochastic processes increase a community's inherent randomness, producing variable microbiomes under identical conditions [7]. Early communities are commonly stochastic [8], with the inherent randomness of dispersal and ecological drift driving composition [9, 10]. In contrast, deterministic processes, focused upon in the

present study, shape communities by selecting for or against specific organisms [11, 12]. Dispersal rates are stochastic if they rely on population size, but species traits and their activity level mean that dispersal can also be deterministic [9]. These complementary processes shape structure by representing extremes along the same continuum, and a process such as dispersal may be equally stochastic and deterministic in a context and habitat-dependent manner [9].

Both abiotic and biotic deterministic processes can influence community assembly. Abiotic factors are chemical or physical environmental components (such as nutrients, pH, temperature, pressure) that affect community composition and function [13, 14]. Meanwhile biotic factors can impose selective pressures related to, or resulting from, living organisms that may affect community composition. Selective pressures associated with biotic interactions across taxa can result in the promotion or inhibition of organisms. For instance, microbial [15, 16] and microbe-higher trophic level (i.e., larger predators) cooperation can increase both participants' abundance. One such example is a copepod's ability to affect environmental community compositions by 'farming' their own microbiome [17]. In contrast, predation promotes the growth of one organism at the expense of another [18, 19], and in some cases facilitating nutrient transfer to successive trophic levels [20]. Both abiotic [21] and biotic [22] factors are dynamic throughout space and time and result in community shifts owing to continuous selective pressures [21, 23, 24].

Selective pressures enact compositional changes through autotrophs (i.e., primary producers) in a bottom–up-dependent manner [25], or through predators in a top–down-dependent manner [26]. Previous studies on environmental microbiology have typically focused on bottom–up controls [4, 27]. Field studies concerning top–down controls are rarer, and bottom–up and top–down selective pressure interaction effects on microbial communities remain largely unexplored [28–31]. Bottom–up microbiome studies commonly report unexplained variance, which could be partially driven by top–down controls [32, 33]. Identifying the contribution of top–down controls to total variance is crucial to better understand community assembly mechanisms. Hence, our study focuses on comparing the effects of bottom–up (i.e., different substrate surface) and top–down (i.e., large predator presence and exclusion via a mesh enclosure) on compositional variance within marine biofilms.

We aim to quantify the influence of top–down and bottom–up controls on community assembly in a model marine biofilm system. We hypothesise that bottom–up controls drive early assembly, while established communities are controlled equally by both bottom–up and top–down mechanisms. Strong early selective pressures during community establishment will result in growth of environment (i.e., substrate) dependent organisms, while a lack of community complexity (i.e., prey richness and availability) decreases predation's influence on composition. Within established communities, nutrient availability will dictate what can grow, while predators will selectively prune targeted organisms, leading to established communities under both top–down and bottom–up controls. To test these hypotheses, we created a model biofilm system using four different substrates (i.e., plastic, glass, tile, wood) to represent a degradability and surface property gradient and thus bottom–up selection. Biofilms were reared in situ under native (non-enclosed) or enclosed (with 100 μm mesh) conditions to model top–down influence by limiting large predator (generally > 100 μm owing to exclusion by the 100 μm mesh) access. Prokaryotic and eukaryotic community successions and composition were monitored via 16S rRNA and 18S rRNA gene amplicon sequencing over a 56-day period. Ultimately, the knowledge derived from this experiment would be applicable across distinct ecosystems, as we assess underlying, rather than habitat specific, processes.

Methods

Sample preparation and collection

Individual 75 × 25 mm substrate slides (glass, tile [i.e., glazed ceramic], plastic [i.e., acryl], and wood [i.e., untreated pine]) were inserted into polyvinyl chloride pipe sections using polyethylene foam and ethyl cyanoacrylate. The substrates and their holders were then either sewn into 25.4 × 30.5 cm 100 μm mesh enclosures to protect against large predators via exclusion or left exposed to the native environment (Supplementary Fig. 1).

Substrates were submerged in the Otago Harbour, New Zealand (45.826678S, 170.641684 E). Samples ($n = 168$) were suspended from a rope using cable ties 80 cm from the seabed, remaining exposed during low-tide but submerged during high-tide. All samples were located in a small geographic area (<30 m^2), 50 metres from shore.

Starting in May 2019, triplicate biofilm sampling was completed on days 7, 14, 19, 28, 42, and 56. However, owing to sample loss ($n = 27$) as a result of the in situ environment, a total of 141 biofilm samples were obtained (Supplementary Table 1). Biofilm was scraped off the entire substrate using a sterile scalpel. Tiles were scraped only on the glazed side. Samples were suspended in 100 μL sterile Milli-Q water and stored at −80 °C until further processing.

Duplicate 1 L water samples were collected 2 metres from both ends of the substrate suspension structure on days 0, 7, 14, 19, 28, 42, and 56. Samples were filtered through a 0.22 μm (diameter = 47 mm) polycarbonate filter prior to freezing and storage at −80 °C until further processing.

All data analysis was carried out using R version 3.6.1 within RStudio [34], and visualised using the ggplot2 package (version 3.2.1) [35] unless otherwise stated. All code and associated files are available at https://github.com/SvenTobias-Hunefeldt/Biofilm_2020/.

DNA extraction and sequencing

DNA was extracted using the Qiagen DNeasy® PowerSoil® Kit (MoBio Laboratories, Carlsbad, CA, USA) according to the manufacturer's protocol. For transport purposes extracted DNA was dehydrated using rotary evaporation in an Eppendorf Concentrator 5301 (Eppendorf, Germany) at 30 °C for 1 h. Community profiles were generated using barcoded 16S (targeting the prokaryotic [bacteria and archaea] V4 region: 515F [5′-NNNNNNNNGTGTGCCA GCMGCCGCGGTAA-3′] and 806R [5′-GGACTACHVG GGTWTCTAAT-3′]) or 18S (targeting the microbial eukaryotic lineage V9 region: 1391f [5′-GTACACACCG CCCGTC-3′] and EukBr [5′-TGATCCTTCTGCAGGTT CACCTAC-3′]) SSU rRNA gene primers as per the Earth Microbiome Project protocol [36]. The 16S primers are biased against *Thaumarchaeota*/*Crenarchaeota* [37] and the SAR11 clade [38], and for Alphaproteobacteria [39], although efforts have since been made to minimise bias [40, 41]. The 18S primers are capable of detecting some 16S rRNA gene targets limiting rare-eukaryote detection, as well as missing many parasitic taxonomic groups [42]. Barcoded samples were then loaded onto separate Illumina MiSeq 2 × 151 bp runs (Illumina, Inc., CA, USA) to produce a total of 13,202,642 and 10,124,722 reads for 16S and 18S runs, with an average of 63,171 and 48,444 per sample and a standard deviation of 28,248 and 18,473. All sequence data from this study has been deposited in NCBI under BioProject PRJNA630803.

16S and 18S rRNA sequencing reads were quality filtered and assigned to amplicon sequencing variants (ASVs) using the dada2 R package (version 1.12.1) and associated pipeline [43]. Taxonomies were assigned in accordance to the dada2 pipeline from the SILVA rRNA reference database (version 132) using the Ribosomal Database Project naive Bayesian classifier method [44]. All data were imported into R for further analysis with the phyloseq R package (version 1.28.0) [45].

The optimum sequencing depth was identified with a custom function utilising functions from the phyloseq, reshape2 (version 1.4.3) [46], plyr (version 1.8.4) [47], base (version 3.6.1) [34], stats (version 3.6.1) [34], and data.table packages (version 1.13.0) [48]. Samples were rarefied 10 times at 11,000 reads using rarefy_even_depth() from the phyloseq package. This depth retains both the maximum number of samples and sequencing depth (Supplementary Fig. 2). Independent rarefactions were combined and underwent sample count transformations using transform_sample_counts() from the phyloseq package to account for multiple rarefactions. To avoid fractional representation of counts all data was rounded to the nearest whole number using the round() command from the stats package. All data analysis used rarefied data unless otherwise stated.

Community analysis

The optimum number of sample clusters based on ASV community composition was assessed with the use of a silhouette and ecotone analysis, using the cluster (version 2.1.0) [49] and EcotoneFinder (version 0.2.0) [50] packages. The EcotoneFinder package was also used to assess group clustering over time [50].

Observed richness was quantified using estimate_richness() from the phyloseq package, and significance analysed using stat_compare_means() from the ggpubr package (version 0.2.4) [51]. Phyloseq package generated NMDS plots assessed beta-diversity, with ggplot2 and ggpubr package adjustments. Clustering was assessed using ADONIS and ANOSIM statistical tests, with the vegan package (version 2.5–6) [52], pairwise PERMANOVA tests identifying significant sample to sample differences. Spearman correlations were used to assess relationships between biofilm age and NMDS1 of the whole community NMDS. Intra-time dissimilarity was calculated with the vegan and phyloseq package, removing self-comparison using the dplyr package (version 0.8.3) [53]. Significant differences between time points were identified with the stats package. The number of shared organisms was calculated using Zeta.decline.mc() from the zetadiv package (version 1.1.1) [54].

Comparisons of means between two groups, such as biofilm succession stages and enclosure conditions, were done with Wilcoxon tests. In the case of more than two groups Kruskal–Wallis tests were used (e.g., differences between biofilm ages and substrates). Pairwise Wilcoxon tests compared individual time points and substrates.

To test for taxonomic composition changes we determined what organisms significantly changed over time using the EdgeR package (version 3.26.8) [55] and an exact test using only biofilm samples. The legend was ordered according to mean relative abundance with the forcats package (version 0.4.0) [56]. All *p* values were false discovery rate adjusted using Bonferroni. A literature search was used to classify phyla as either autotrophs [57–60], heterotrophs [61–72], mixotrophs [63, 64, 73, 74], or unknown if the literature was lacking. Unknown taxonomies were excluded due to their low abundance (Supplementary Table 1), and unknown role in predator-prey dynamics.

Rare taxa (i.e., below 1% of the total abundance) were identified and combined into one group for ease of

visualisation using the plyr package and standard error, standard deviation and the 95% confidence interval calculated with the Rmisc and dplyr packages.

Results

Biofilm community compositions clustered into two stages

Silhouette analyses were used to identify the optimum number of clusters that samples could be grouped into based on ASV abundance similarities. Prokaryotes were best divided into two groups (silhouette width = 0.43), predominantly based on community age, whereas eukaryotic groupings could not be reliably identified (silhouette width < 0.4). Although three eukaryotic groups resulted in the highest average silhouette width (Supplementary Figure 3), average silhouette widths below 0.4 are considered unreliable [75]. Ecotone analyses compared sample amplicon sequence variants (ASV) abundances to identify both the optimum number of sample clusters and when communities changed for both prokaryotes and eukaryotes (Fig. 1). Two clusters corresponded well with Sorensen dissimilarity patterns (Fig. 1c, d), where only 2 (day 7 and 14 for prokaryotes) and 1 (day 7 for eukaryotes) out of six time points were classified as early (Fig. 1e, f). Richness (the number of unique ASVs within a sample) significantly increased 1.9-fold with biofilm age (Kruskal–Wallis, $\chi^2 > 19$, $p < 0.01$), from the early to late stage (Supplementary Figure 4A, B, Wilcoxon, $\chi > 390$, $p < 0.01$). Pairwise Wilcoxon analyses further confirmed richness differences between succession stages (Wilcoxon, Supplementary Table 2A) with the exceptions of prokaryote day 14–19 and eukaryote day 7–14 pairings, with non-significant late successional stage intra-stage differences (Wilcoxon, $p > 0.6$, Supplementary Table 2A). Compositional patterns also exhibited stage significant grouping, both when comparing group means (ANOSIM, $R = 0.67$, $p < 0.01$) and when taking variability into account (ADONIS, $R^2 = 0.13$, $p < 0.01$). Communities stabilised from day 19–42 (prokaryotes) and 14–42 (eukaryotes) (Supplementary Fig. 4C), with early-stage samples sharing fewer ASVs across substrates (Supplementary Fig. 4D). Thus, prokaryotic and eukaryotic communities across all treatments clustered into two significantly distinct succession stages: early and late.

Community successions lead to convergence across substrates

Community successions were detected in response to biofilm age (Table 1, Fig. 2). Biofilm age significantly correlated with NMDS1 (Fig. 2; Spearman, $rho > 0.66$, $p < 0.01$), and both maturation and sequential clustering coincided with community convergence across substrates. Community turnover, in the form of significant dissimilarity differences between subsequent time points, decreased with biofilm age (Spearman, $rho = 0.89$ [prokaryotes $p < 0.01$] and 0.66 [eukaryotes $p = 0.018$]; Supplementary Fig. 5). Pairwise dissimilarity comparisons showed significant community turnover (Wilcoxon, $p < 0.05$, Supplementary Table 2B), with exceptions (prokaryotic day 19–28 and 42–56 pairs, and all possible eukaryotic pairings between days 19, 28, 42, and 56). Community variance within a single timepoint decreased over time for prokaryotes (31%; Spearman, $rho = -0.71$, $p = 0.01$) and eukaryotes (9.1%; Spearman, $rho = -0.47$, $p = 0.13$), especially when comparing early to late time points, such as day 7–56 (Supplementary Fig. 4C; Wilcoxon, $p < 0.01$, Supplementary Table 2C). However, the decreases in prokaryotic variance were more pronounced than for eukaryotes (Supplementary Fig. 4C). Both prokaryotes and eukaryotes showed increased ASV sharing across substrates over time (Supplementary Fig. 4D). The number of shared ASVs across substrates increased from 1.8 (prokaryotes) and 3.3% (eukaryotes) to 22 and 9.4% of the total ASV number respectively. Enclosed prokaryotic communities (excluding organisms >100 µm) matured at an increased rate, with differences quantified as an average dissimilarity increase to the initial composition of 0.02% per day. Over 56 days the difference in community succession turnover lead to a maximum dissimilarity of 11.2%, whereas, mean dissimilarity between all day 56 prokaryotic communities was 61%.

Anosim and adonis tests assessed how well community composition and variance could be explained by either substrate or enclosure condition. A gradual transition from bottom–up to top–down control was associated with community convergence, although more prokaryotic than eukaryotic dissimilarity variation could be explained (Table 1, Supplementary Fig. 6). Substrates determined early clustering (Table 1, Fig. 2), with distinct wood-associated microbial compositions (pairwise multivariate analysis of variance, $p < 0.01$, Supplementary Table 2D), although enclosure status still played a significant role (>7.6% of variance; Table 1). Late prokaryotic community variance could be primarily attributed to enclosure differences (Table 1, Supplementary Figure 7) with minimal substrate dependent effects (Fig. 2). Meanwhile, late eukaryotic compositions were determined by time, although enclosure conditions explained more community variance than substrates (Table 1).

Enclosure conditions determine late community richness, with minor substrate effects

Enclosures increased late stage richness by twofold (Wilcoxon, $p < 0.01$) (Fig. 3, Supplementary Figure 4A, B)
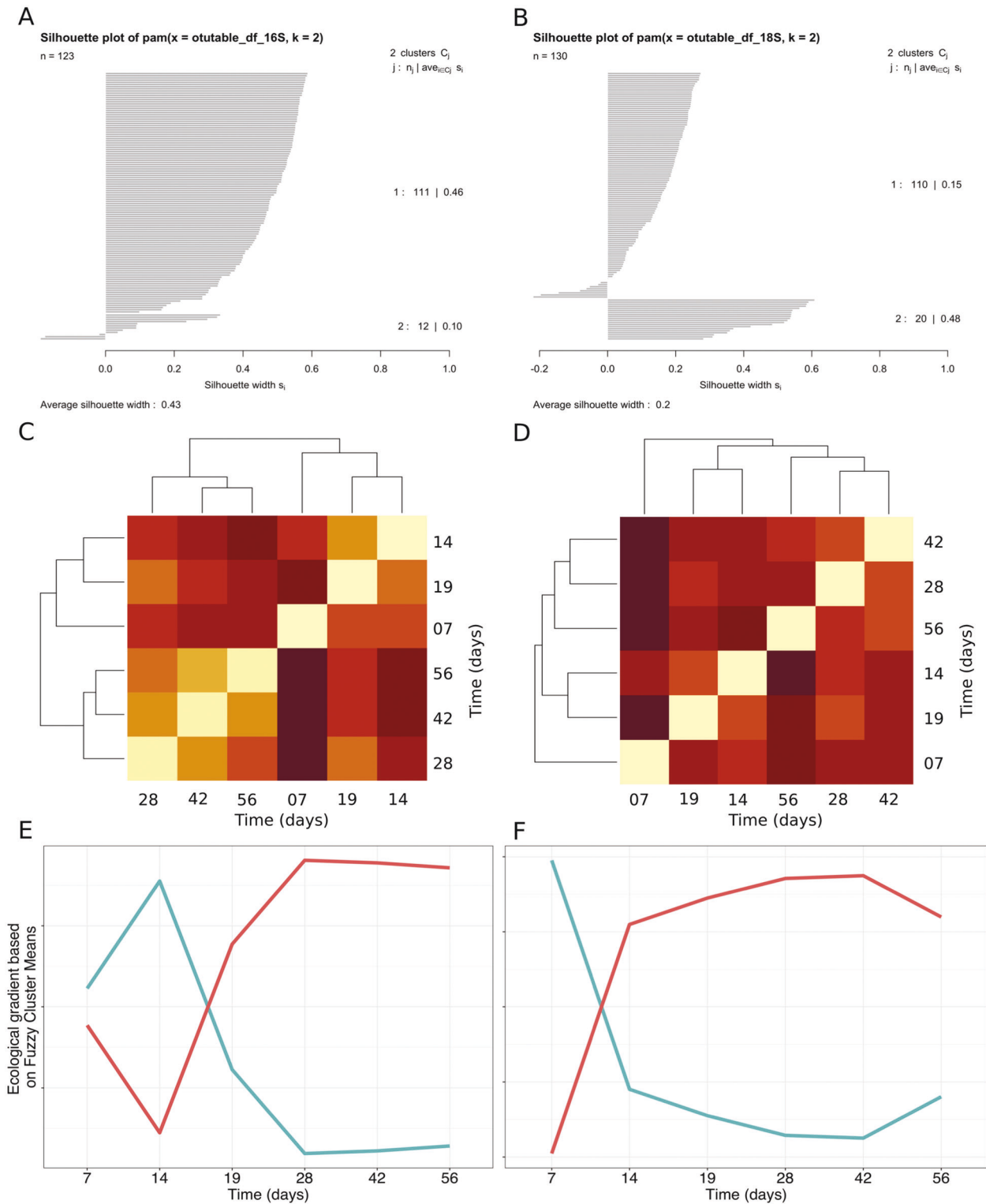
Fig. 1 Two development stages identified through silhouette and ecotone analysis for prokaryotic (left) and eukaryotic (right) communities. The optimum number of groups was determined using a silhouette **a**–**b** and ecotone transition zone **c**–**f** analysis based on both prokaryotic **a**, **c**, **e** and eukaryotic **b**, **d**, **f** ASV abundances. Sample dissimilarity was tested with Sorensen dissimilarity, and the best fitting number of groups based on both the silhouette analysis and heatmap was used to identify the transition zones. A darker colour represent increased dissimilarity, and ecotone grouping colours represent the two identified groups with the average species abundance and biofilm age depicted on the *y* axis and *x* axis.

Table 1 ANOSIM and ADONIS tests compare time, substrate, and enclosure correlations over time on biofilm prokaryotes and eukaryotes.

| Organism	Test	Biofilm development stage	Variable	R/R^2	p value
Prokaryotes	Anosim	Early	Time	0.3	<0.01
			Substrate	0.5	<0.01
			Enclosure status	0.19	<0.01
		Late	Time	0.3	<0.01
			Substrate	0.19	<0.01
			Enclosure status	0.41	<0.01
	Adonis	Early	Time	0.11	<0.01
			Substrate	0.24	<0.01
			Enclosure status	0.08	<0.01
			Substrate×enclosure status	0.08	<0.01
		Late	Time	0.19	<0.01
			Substrate	0.12	<0.01
			Enclosure status	0.12	<0.01
			Substrate×enclosure status	0.05	<0.01
Eukaryotes	Anosim	Early	Time	NA	
			Substrate	0.34	<0.01
			Enclosure status	0.52	<0.01
		Late	Time	0.32	<0.01
			Substrate	0.06	<0.01
			Enclosure status	0.23	<0.01
	Adonis	Early	Time	NA	
			Substrate	0.28	<0.01
			Enclosure status	0.15	<0.01
			Substrate×enclosure status	0.16	0.09
		Late	Time	0.16	<0.01
			Substrate	0.05	<0.01
			Enclosure status	0.07	<0.01
			Substrate×enclosure status	0.04	<0.01
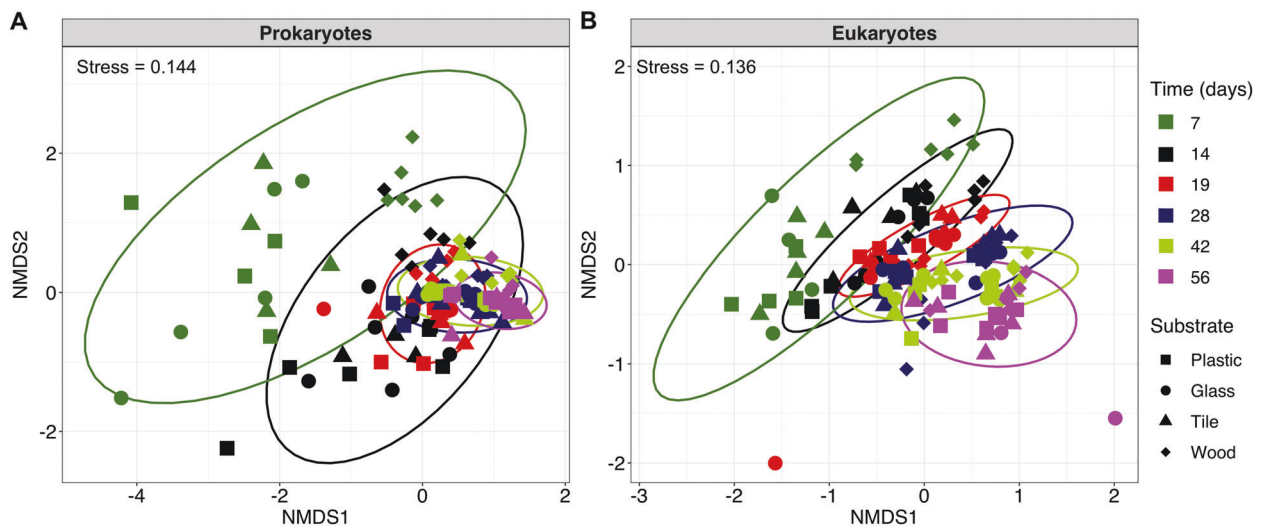
Fig. 2 Microbial biofilm beta-diversity by time. NMDS plots show prokaryotes **a** and eukaryotes **b**, ellipses depict the 95% confidence interval grouping effects of time with biofilm age represented as different colours (days 7, 14, 19, 28, 42, and 56 depicted as olive, black, red, navy, green, and magenta). Substrates are depicted with different shapes, diamonds represent wood whereas the square, circle, and triangle represent plastic, glass, and tile. Stress is included in the upper left corner of individual plots.
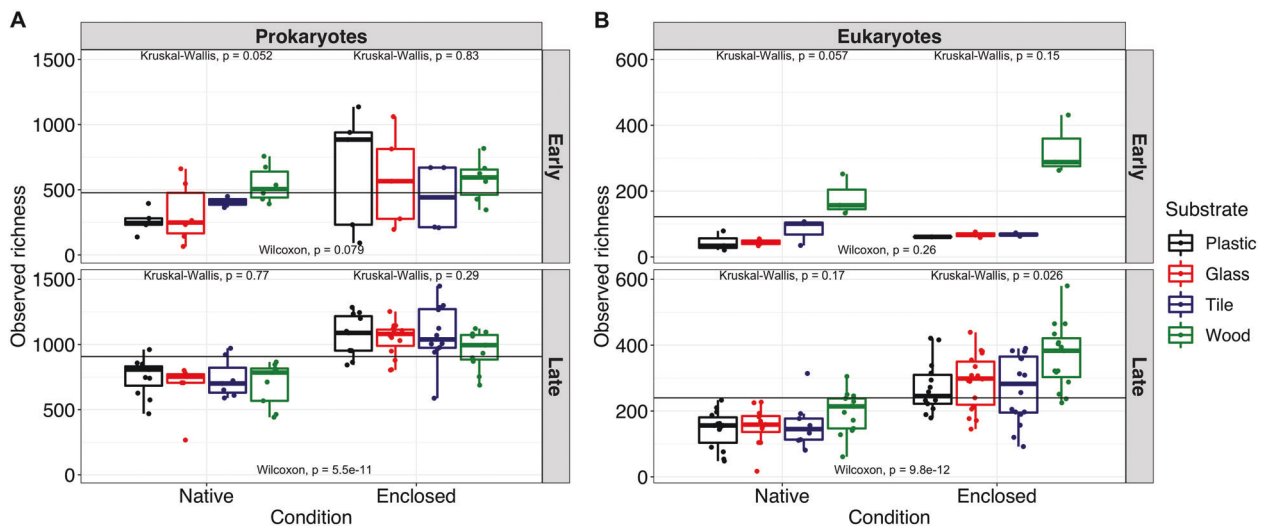
Fig. 3 Prokaryotic and eukaryotic observed richness is enclosure specific in a stage dependent manner. Marine in situ biofilm species richness for both prokaryotes **a** and eukaryotes **b** is shown by developmental stage grouping. The black horizontal line represents the organisms and stage specific richness mean, whereas colours separate the different substrates. Plastic, glass, tile, and wood is depicted in black, red, navy, and green. Wilcoxon tests assessed the significance of stage specific enclosure differences, and Kruskal–Wallis tests identified the significance of substrate effects in a stage and enclosure specific manner.

whereas early communities remained unaffected (Wilcoxon, prokaryote $p = 0.08$, eukaryote $p = 0.26$). Early wood-associated eukaryotes displayed significantly increased richness compared to all other substrates (Kruskal–Wallis, $p < 0.01$; pairwise Wilcoxon, $p < 0.05$, Supplementary Table 2E). Otherwise substrate-specific differences were enclosure dependent: 100–250 more ASVs were detected within early native wood prokaryotic and late enclosed eukaryotic communities compared with more inert substrates (Fig. 3). On average prokaryotic wood communities contained 46 less ASVs than inert substrates, whereas eukaryotic ASV numbers increased by 79 (Fig. 3). Prokaryotic substrate richness differences were only significant when wood contained an increased number of ASVs compared with inert substrates, such as under native early conditions. Overall, enclosure conditions exerted significantly more pressure on late communities. Early richness was not consistently driven by either the enclosure or substrate, whereas late richness differences were primarily determined by enclosure condition, with only minor substrate effects (Fig. 3).

Shifts in dominant taxa reflect changes in selective pressures

Phylum level changes were observed in response to a switch from bottom–up to top–down control mechanisms (Fig. 4). Early communities differed primarily by substrates (Table 1; Supplementary Figure 6); wood displayed more Proteobacteria (34%) and Euglenozoa (41%), and less autotrophs (25%) compared with inert substrates (Supplementary Table 3). Enclosure effects became increasingly

important over time, until the enclosure condition primarily determined late community variance (Supplementary Figure 6), with no consistent substrate effect. Enclosed biofilms were dominated by mixotrophs and heterotrophs while native conditions contained more autotrophs. Late enclosed community autotroph relative abundance was half that of native conditions. Relative Ochrophyta abundance decreased from >36% to ~15% across all substrates. Meanwhile, relative Cyanobacteria abundance increased in glass, tile, and acyl plastic from <30% to >53% from days 7 to 14, and then decreased to ~17%, whereas wood Cyanobacteria abundance rose by 10%. However, with autotroph decreases came mixotroph and heterotroph increases. Over 56 days Proteobacteria relative abundance increased by a mean 16.7%, whereas Bacteroidetes, Ciliophora, and Arthropoda relative abundance rose by 11%, 21%, and 49%, respectively (Supplementary Table 3). Within native biofilms Bacteroidetes, Ciliophora, and Arthropoda stayed <25% relative abundance, whereas Cyanobacteria increased by 21% within wood and remained >45% within all other substrates. Early autotroph–heterotroph balances corresponded to substrate differences. Subsequent autotroph–heterotroph distributions shifted and became enclosure dependent. Phylum level community trends were conserved at the genus level (Supplementary Figs. 8, 9).

Discussion

Our results show that the analysis of bottom–up selective pressures (i.e., substrate differences) are sufficient to determine
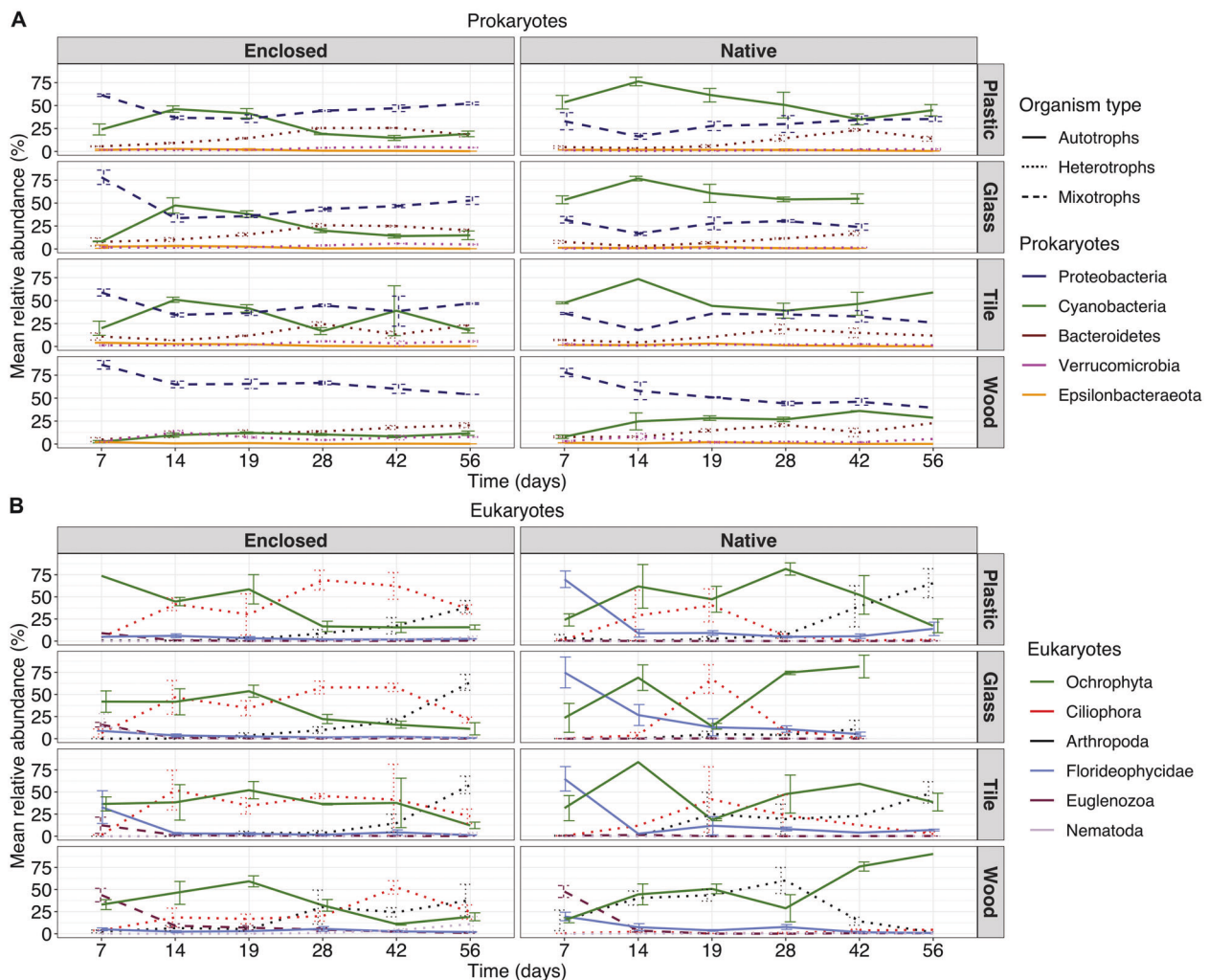
Fig. 4 Significant phylum changes in response to biofilm age. The mean relative abundance of significantly prokaryotic **a** and eukaryotic **b** phyla correlated with biofilm age are depicted with enclosed communities on the left and native (non-enclosed) on the right in a substrate dependent manner. The type of line (solid, dotted, and dashed) represent the three main types of organisms; autotrophs, heterotrophs, and mixotrophs. Mean relative abundance was calculated from pooled significantly correlated taxa and error bars represent the standard error of the mean abundance based on biological replicates.

the majority of community variance when assessing drivers of early unstable communities, but accounting for top–down selective pressures (i.e., using a 100 μm mesh enclosure to exclude large organisms) captures more variance in established communities. We created a community assembly model (Fig. 5) describing the effect of sequential bottom–up and top–down control over time. Following substrate colonisation, growth resulted in distinct compositions likely owing to nutrient availability (i.e., degradable vs non-degradable substrates). Early bottom–up control weakens leading to community convergence over time across all substrates with late compositions modified by top–down selective pressures. Our work thus addresses some of the controversy in prior microbial ecology studies by discussing the relative effects of bottom–up and top–down selective pressures over time.

Stochasticity and substrate differences drive early community compositions

Early community stochasticity is common within microbial models [76], but dependent on resource supply within macrobial studies [10]. Stochasticity has a large role during dispersal, controlling early community establishment [9]. Our study controlled for uneven dispersal by limiting geographical range. However, early communities remained highly stochastic, reflected in high confidence intervals, turnover rates, and intra-age dissimilarities. Selection also has a role during community establishment [7], particularly substrate surface attachment and mesh enclosure size exclusion. Early colonisers must be capable of adhering to the surface to establish the biofilm, just as enclosed conditions
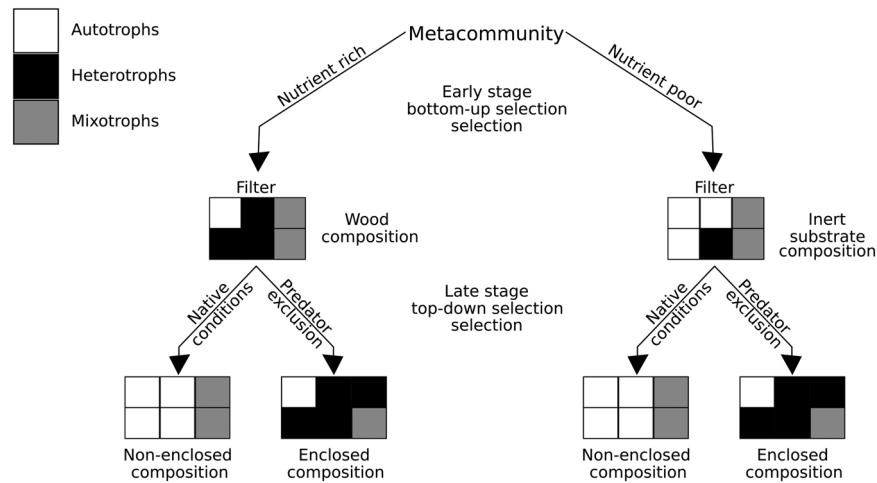
Fig. 5 Microbial biofilm community assembly is divided into discrete stages associated with distinct compositions and selective pressures. Communities are a subset from the environmental organism pool known as the metacommunity and filtered in response to a selective pressure. Selective pressures filter for distinct community compositions. First, bottom–up (early stage) substrate differences and then top–down (late stage) enclosure status determine biofilm community composition, with decreased bottom–up differences owing to top–down filtering.

dictate that they must be <100 μm. The exclusion of large organisms (e.g., macro-algae and macro-eukaryotes) did not play a large role during community establishment, as they are not primary settlers, and instead prefer established and complex communities [77], as such size-based large predator exclusion was chosen as our top–down control.

Following settlement, deterministic factors become increasingly important in determining community composition, whereas stochastic factors retain an important but secondary role [10, 78]. Wood-associated biofilms consistently contained more ASVs compared with inert substrates. Retainment of terrestrial microbes could have contributed to the noted high early richness on wooden substrates, however wood-associated richness (both prokaryotic and eukaryotic) remained consistently high throughout the study. Therefore, early-stage wood richness increases are more likely owing an inherent property of wood, such as an increased roughness and degradable organic carbon, rather than microbes harboured by the substrate [79, 80]. Grooves within rough surfaces increase the colonisation surface area, and provide protection from shear stress and large predators [81]. A significant biomass increase on wood could have resulted in the lack of significant late prokaryotic substrate effects, as less abundant organisms are excluded in uneven communities during rarefaction. However, it is important to note that substrates displayed significant eukaryotic richness differences to each other throughout the study.

Wood contained significantly dissimilar prokaryote and eukaryote communities compared with other substrates, under both enclosed and native conditions. Degradable organic carbon within wood (lignocellulose) could be acting as an environmental filter for mixotrophic and heterotrophic organisms (i.e., *Proteobacteria* and *Bacteroidetes* [67, 82]). Inert substrates (i.e., plastic, glass, and tile) cannot be degraded in the same manner, and their early communities were instead primarily composed of autotrophs.

Community compositions converged with age

Stochastic fluctuations throughout time and genetic variation (drift and diversification) are inherent properties of time-dependent ecological studies [7], leading to divergent [83–85] or convergent communities [5, 84, 86]. Our study identified prokaryotic and eukaryotic community convergence over time, with increased numbers of shared organisms, and decreased turnover rates and variability associated with established ecosystems [87, 88]. Convergence likely arose owing to preconditioning (i.e., selecting for organisms with a history of surface attachment from a single population pool) [89] and sequential compositional changes over time selecting for specific taxa [12].

Based on the evidence, we conclude that the more unpredictable early communities converge into stable late communities. Community stabilisation occurs in response to both primary [9] and secondary [76] successions. Therefore, our observations regarding primary succession can also be applied to secondary successions.

Enclosure differences control diversity and late community compositions

Enclosure effects could be owing to a multitude of factors, such as the nutrient supply, shear stress, light availability,

and differences in predation by large organisms. Enclosed conditions can experience a decreased flow rate potentially containing organic nutrients, which would lead to an increased autotroph abundance. Instead autotrophs (i.e., cyanobacteria, florideophycidae, and ochrophyta) made up less of the enclosed communities. Light availability limitations could explain this, with growth on the mesh enclosure and the mesh providing shade [90]. Growth on the mesh enclosure would decrease autotroph abundance over time, as mesh community density increases. However, cyanobacteria and ochrophyta relative abundance peaks at day 14 and 19, suggest that light limitations associated with growth on the mesh may not be as important as other compositional drivers. The inherent mesh shade effect would only weakly contribute to compositional differences, as early community variance was primarily associated with substrate differences. Sheer stress acts through biomass removal [91], which has no effect on relative abundances. High stress has also been shown to decrease biofilm maturation rates [92], but neither enclosure-dependent prokaryotic and eukaryotic community differences could be solely attributed to maturation rate differences. Therefore, enclosure differences are more likely owing to predation rather than other enclosure associated effects.

Predation can modify net community composition and richness through the direct or indirect selection of specific lineages [93, 94] (e.g., Arthropoda selection against Ciliophora [95]). Our study identified decreased diversity in response to large organism predation. Although substrate effects could be identified they remained predominantly enclosure condition specific (e.g., wood showed increased richness within early predated prokaryotes and late enclosed eukaryotes).

In situ conditions exhibit a much larger variety of predatory organisms, opposed to laboratory conditions where specific predators are introduced to the system. It is therefore challenging to link microbial community changes to specific predators under in situ conditions. Identifying interactions between microbial taxa within a biofilm is easier owing to the closer proximity. We identified a series of inverse relationships between organisms with a history of predation. The prime example of this is the potential consumption chain from ochrophyta (specifically diatoms) to ciliophora [96], and arthropoda consuming ciliophora [95].

Large predators affect late communities to a greater extent than their early counterparts. Early communities lack the inherent complexity and resources to sustain large predator and heterotrophic organism abundances unless a source of organic carbon is available [77]. Enclosed conditions displayed an inverse relationship between prokaryotic and eukaryotic heterotrophs and autotrophs over time (Fig. 5), as heterotrophs drove their prey below detectable

limits [62, 66, 67]. Meanwhile native conditions experienced increased autotroph abundance owing to heterotroph predation by large predators (Fig. 5). The preference for heterotrophs could be owing to their increased stoichiometric stability and closer ratio matches compared with autotrophs. Autotrophic stoichiometries reflect environment ratios, whereas heterotrophs are strongly homoeostatic [97] with lower C to P ratios [97, 98]. Predators prefer the ingestion of close stoichiometric matches [99], and have even been shown to reject nitrogen-depleted prey [100]. Heterotrophic preference also explains the close relationships between heterotrophs and higher trophic levels [101], such as the previously identified inverse relationship between Ciliophora (a heterotroph) and Arthropoda (a eukaryotic predator) [95].

Conclusion

We identified a switch from bottom–up to top–down control linked to community maturation. This switch in primary selective pressure highlights the community selection of primary colonisers, to the emergence of stable and convergent mature communities modified by the presence of large predators (Fig. 5). Predation selectively removes organisms, potentially using nutritional value as a criteria. The integration of a top–down control allowed for the explanation of more variance than a sole bottom–up focus. Hence, increased importance should be placed on top–down controls, particularly for studies concerning stable late communities. The integration of both bottom–up and top–down selective pressures in the field of microbial ecology leads to a better understanding of assembly mechanism. Studies that assess the underlying processes ultimately identify not only habitat specific community compositions, but also what lead to these habitat compositional patterns.

Data availability

The sequence data from this study have been deposited in NCBI under BioProject PRJNA630803. All data generated and/or analysed during the study is available within the GitHub repository, https://github.com/SvenTobias-Hunefeldt/Biofilm_2020/.

Compliance with ethical standards

References

1. Wade W. Unculturable bacteria - the uncharacterized organisms that cause oral infections. J R Soc Med. 2002;95:81–3.
2. Stewart EJ. Growing unculturable bacteria. J Bacteriol. 2012;194:4151–60.
3. Estes JA, Palmisano JF. Sea otters: their role in structuring nearshore communities. Science. 1974;185:1058–60.
4. Rajput R, Pokhriya P, Panwar P, Arunachalam A, Arunachalam K. Soil nutrients, microbial biomass, and crop response to organic amendments in rice cropping system in the Shiwaliks of Indian Himalayas. Int J Recycl Org Waste Agric. 2019;8:73–85.
5. Ofiţeru ID, Lunn M, Curtis TP, Wells GF, Criddle CS, Francis CA, et al. Combined niche and neutral effects in a microbial wastewater treatment community. Proc Natl Acad Sci USA. 2010;107:15345–50.
6. Pereira e Silva MC, Dias ACF, van Elsas JD, Salles JF. Spatial and temporal variation of archaeal, bacterial and fungal communities in agricultural soils. PLoS ONE. 2012;7:e51554.
7. Nemergut DR, Schmidt SK, Fukami T, O'Neill SP, Bilinski TM, Stanish LF, et al. Patterns and processes of microbial community assembly. Microbiol Mol Biol Rev. 2013;77:342–56.
8. Evans S, Martiny JBH, Allison SD. Effects of dispersal and selection on stochastic assembly in microbial communities. ISME J. 2017;11:176–85.
9. Zhou J, Ning D. Stochastic community assembly: does it matter in microbial ecology? Microbiol Mol Biol Rev. 2017;81:e00002-17.
10. Dini-Andreote F, Stegen JC, Van Elsas JD, Salles JF. Disentangling mechanisms that mediate the balance between stochastic and deterministic processes in microbial succession. Proc Natl Acad Sci USA. 2015;112:E1326–32.
11. Ju F, Xia Y, Guo F, Wang Z, Zhang T. Taxonomic relatedness shapes bacterial assembly in activated sludge of globally distributed wastewater treatment plants. Environ Microbiol. 2014;16:2421–32.
12. Wang J, Shen J, Wu Y, Tu C, Soininen J, Stegen JC, et al. Phylogenetic beta diversity in bacterial assemblages across ecosystems: Deterministic versus stochastic processes. ISME J. 2013;7:1310–21.
13. Price PB, Sowers T. Temperature dependence of metabolic rates for microbial growth, maintenance, and survival. Proc Natl Acad Sci USA. 2004;101:4631–6.
14. Bartlett DH. Pressure effects on in vivo microbial processes. Biochim Biophys Acta. 2002;1595:367–81.
15. Damore JA, Gore J. Understanding microbial cooperation. J Theor Biol. 2012;299:31–41.
16. Knowlton N, Rohwer F. Multispecies microbial mutualisms on coral reefs: the host as a habitat. Am Nat. 2003;162:S51–62.
17. Shoemaker KM, Duhamel S, Moisander PH. Copepods promote bacterial community changes in surrounding seawater through farming and nutrient enrichment. Environ Microbiol. 2019;21:3737–50.
18. Jürgens K, Matz C. Predation as a shaping force for the phenotypic and genotypic composition of planktonic bacteria. Antonie van Leeuwenhoek. 2002;81:413–34.
19. Sherr EB, Sherr BF. Significance of predation by protists in aquatic microbial food webs. Antonie van Leeuwenhoek. 2002;81:293–308.
20. Azam F, Fenchel T, Field J, Gray J, Meyer-Reil L, Thingstad F. The ecological role of water-column microbes in the sea. Mar Ecol Prog Ser. 1983;10:257–63.
21. Gilbert JA, Steele JA, Caporaso JG, Steinbrück L, Reeder J, Temperton B, et al. Defining seasonal marine microbial community dynamics. ISME J. 2012;6:298–308.
22. Pacheco AR, Segrè D. A multidimensional perspective on microbial interactions. FEMS Microbiol Lett. 2019;366:fnz125.
23. Coleman ML, Chisholm SW. Ecosystem-specific selection pressures revealed through comparative population genomics. Proc Natl Acad Sci USA. 2010;107:18634–9.
24. Freestone AL, Carroll EW, Papacostas KJ, Ruiz GM, Torchin ME, Sewall BJ. Predation shapes invertebrate diversity in tropical but not temperate seagrass communities. J Anim Ecol. 20201;89:323–33.
25. Hutchinson GE. Homage to santa rosalia or why are there so many kinds of animals? Am Nat. 1959;93:145–59.
26. Holt AR, Davies ZG, Tyler C, Staddon S. Meta-analysis of the effects of predation on animal prey abundance: evidence from UK vertebrates. PLoS ONE. 2008;3:e2400.
27. del Giorgio PA, Bouvier TC. Linking the physiologic and phylogenetic successions in free-living bacterial communities along an estuarine salinity gradient. Limnol Oceanogr. 2002;47:471–86.
28. Lee CK, Laughlin DC, Bottos EM, Caruso T, Joy K, Barrett JE, et al. Biotic interactions are an unexpected yet critical control on the complexity of an abiotically driven polar ecosystem. Commun Biol. 2019;2:62.
29. Gasol JM. A framework for the assessment of top-down vs bottom up control of heterotrophic nanoflagellate abundance. Mar Ecol Prog Ser. 1994;113:291–300.
30. Berdjeb L, Ghiglione JF, Jacquet S. Bottom-up versus top-down control of hypo-and epilimnion free-living bacterial community structures in two neighboring freshwater lakes. Appl Environ Microbiol. 2011;77:3591–9.
31. Grattepanche J-D, Juarez DL, Wood CC, McManus GB, Katz LA. Top-down and bottom-up effects on microbial eukaryotic diversity inferred from molecular analyses of microcosm experiments. PLoS ONE. 2019;14:e0215872.
32. Lami R, Ghiglione JF, Desdevises Y, West NJ, Lebaron P. Annual patterns of presence and activity of marine bacteria monitored by 16S rDNA-16S rRNA fingerprints in the coastal NW Mediterranean Sea. Aquat Micro Ecol. 2009;54:199–210.
33. Scepanovic P, Hodel F, Mondot S, Partula V, Byrd A, Hammer C, et al. A comprehensive assessment of demographic, environmental, and host genetic associations with gut microbiome diversity in healthy individuals. Microbiome. 2019;7:130.
34. R Core Team. R: A Language and Environment for Statistical Computing. Vienna, Austria; 2019. Available from: http://www.r-project.org/.
35. Wickham H ggplot2: Elegant Graphics for Data Analysis. Springer-Verlag New York; 2016. Available from: http://ggplot2.org.
36. Thompson LR, Sanders JG, McDonald D, Amir A, Ladau J, Locey KJ, et al. A communal catalogue reveals Earth's multi-scale microbial diversity. Nature. 2017;551:457–63.
37. Hugerth LW, Wefer HA, Lundin S, Jakobsson HE, Lindberg M, Rodin S, et al. DegePrime, a program for degenerate primer design for broad-taxonomic-range PCR in microbial ecology studies. Appl Environ Microbiol. 2014;80:5116–23.
38. Morris RM, Rappé MS, Connon SA, Vergin KL, Siebold WA, Carlson CA, et al. SAR11 clade dominates ocean surface bacterioplankton communities. Nature. 2002;420:806–10.
39. Thijs S, De Beeck MO, Beckers B, Truyens S, Stevens V, Van Hamme JD, et al. Comparative evaluation of four bacteria-specific primer pairs for 16S rRNA gene surveys. Front Microbiol. 2017;8:494.

40. Apprill A, Mcnally S, Parsons R, Weber L. Minor revision to V4 region SSU rRNA 806R gene primer greatly increases detection of SAR11 bacterioplankton. Aquat Micro Ecol. 2015;75:129–37.

41. Parada AE, Needham DM, Fuhrman JA. Every base matters: assessing small subunit rRNA primers for marine microbiomes with mock communities, time series and global field samples. Environ Microbiol. 2016;18:1403–14.

42. Kounosu A, Murase K, Yoshida A, Maruyama H, Kikuchi T. Improved 18S and 28S rDNA primer sets for NGS-based parasite detection. Sci Rep. 2019;9:1–12.

43. Callahan BJ, McMurdie PJ, Rosen MJ, Han AW, Johnson AJA, Holmes SP. DADA2: high-resolution sample inference from Illumina amplicon data. Nat Methods. 2016;13:581–3.

44. Wang Q, Garrity GM, Tiedje JM, Cole JR. Naïve Bayesian classifier for rapid assignment of rRNA sequences into the new bacterial taxonomy. Appl Environ Microbiol. 2007;73:5261–7.

45. McMurdie PJ, Holmes S. Phyloseq: an R package for reproducible interactive analysis and graphics of microbiome census data. PLoS ONE. 2013;8:e61217.

46. Wickham H. Reshaping data with the reshape package. J Stat Softw. 2007;21:1–20.

47. Wickham H. The split-apply-combine strategy for data analysis. J Stat Softw. 2011;40:1–29.

48. Dowle M, Srinivasan A. data.table: extension of 'data.frame'. R Packag version 1126. 2019.

49. Gentle JE, Kaufman L, Rousseeuw PJ. Finding droups in data: an introduction to cluster analysis. Biometrics. 1991;47:788.

50. Bagnaro A, Baltar F, Brownstein G, Lee WG, Morales SE, Pritchard DW, et al. Reducing the arbitrary: fuzzy detection of microbial ecotones and ecosystems – focus on the pelagic environment. Environ Microbiome. 2020;15:16.

51. Kassambara A. ggpubr: "ggplot2" Based Publication Ready Plots. 2019. Available from: https://cran.r-project.org/package= ggpubr.

52. Oksanen J, Blanchet FG, Friendly M, Kindt R, Legendre P, McGlinn D, et al. vegan: Community Ecology Package. 2019; Available from: http://doi.acm.org/10.1145/2037556.2037605% 5Cnftp://ftp3.ie.freebsd.org/pub/cran.r-project.org/web/packa ges/vegan/vignettes/intro-vegan.pdf.

53. Wickham H, François R, Henry L, Müller K. dplyr: A Grammar of Data Manipulation. 2019. Available from: https://cran.r- project.org/package=dplyr.

54. Latombe G, McGeoch MA, Nipperess DA, Hui C. zetadiv: Functions to Compute Compositional Turnover Using Zeta Diversity. 2018. p. R package version 1.1.1.

55. Robinson MD, McCarthy DJ, Smyth GK. edgeR: a bioconductor package for differential expression analysis of digital gene expression data. Bioinformatics. 2010;26:139–40.

56. Wickham H. forcats: Tools for Working with Categorical Variables (Factors). 2019. Available from: https://cran.r-project.org/ package=forcats.

57. Waite DW, Vanwonterghem I, Rinke C, Parks DH, Zhang Y, Takai K, et al. Comparative genomic analysis of the class Epsilonproteobacteria and proposed reclassification to epsilonbacteraeota (phyl. nov.). Front Microbiol. 2017;8:682.

58. Bhatnagar M, Bhatnagar A. Diversity of polysaccharides in cyanobacteria. In: Microbial Diversity in Ecosystem Sustainability and Biotechnological Applications. Singapore: Springer Singapore; 2019 [cited 2019 Jul 25]. p. 447–96. Available from: http://link.springer.com/10.1007/978-981-13-8315-1_15.

59. Sukenik A, Zohary T, Padisák J. Cyanoprokaryota and other prokaryotic algae. In: Encyclopedia of Inland Waters. Elsevier Inc.; 2009. p. 138–48.

60. Cavalier-Smith T. Kingdom Chromista and its eight phyla: a new synthesis emphasising periplastid protein targeting, cytoskeletal and periplastid evolution, and ancient divergences. Protoplasma. 2018;255:297–357.

61. Wexler HM. Bacteroides: the good, the bad, and the nitty-gritty. Clin Microbiol Rev. 2007;20:593–621.

62. Thomas F, Hehemann JH, Rebuffet E, Czjzek M, Michel G. Environmental and gut bacteroidetes: the food connection. Front Microbiol. 2011;2:93.

63. Carere CR, Hards K, Houghton KM, Power JF, McDonald B, Collet C, et al. Mixotrophy drives niche expansion of verrucomicrobial methanotrophs. ISME J. 2017;11:2599–610.

64. Taylor WD, Sanders RW. Protozoa. In: Ecology and Classification of North American Freshwater Invertebrates. Elsevier Inc.; 2010. p. 49–90.

65. Spring S, Bunk B, Spröer C, Schumann P, Rohde M, Tindall BJ, et al. Characterization of the first cultured representative of Verrucomicrobia subdivision 5 indicates the proposal of a novel phylum. ISME J. 2016;10:2801–16.

66. Thorp JH, Rogers DC. Introduction to the Phylum Arthropoda. In: Thorp and Covich's Freshwater Invertebrates: Ecology and General Biology: Fourth Edition. Elsevier Inc.; 2014. p. 591–7.

67. Smith MW, Herfort L, Fortunato CS, Crump BC, Simon HM. Microbial players and processes involved in phytoplankton bloom utilization in the water column of a fast-flowing, river-dominated estuary. Microbiologyopen. 2017;6:e00467.

68. Fujio-Vejar S, Vasquez Y, Morales P, Magne F, Vera-Wolf P, Ugalde JA, et al. The gut microbiota of healthy Chilean subjects reveals a high abundance of the phylum Verrucomicrobia. Front Microbiol. 2017;8:1221.

69. Majdi N, Traunspurger W. Free-living nematodes in the freshwater food web: a review. 2015;47:28–44.

70. Dong Y, Geng J, Liu J, Pang M, Awan F, Lu C, et al. Roles of three TonB systems in the iron utilization and virulence of the Aeromonas hydrophila Chinese epidemic strain NJ-35. Appl Microbiol Biotechnol. 2019;103:4203–15.

71. Lee KC, Webb RI, Janssen PH, Sangwan P, Romeo T, Staley JT, et al. Phylum Verrucomicrobia representatives share a compartmentalized cell plan with members of bacterial phylum Planctomycetes. BMC Microbiol. 2009;9:5.

72. Yeates GW, Bongers T, De Goede RGM, Freckman DW, Georgieva SS. Feeding habits in soil nematode families and genera-an outline for soil ecologists. J Nematol. 1993;25:315–31.

73. Suyama T, Shigematsu T, Suzuki T, Tokiwa Y, Kanagawa T, Nagashima KVP, et al. Photosynthetic apparatus in Roseateles depolymerans 61A is transcriptionally induced by carbon limitation. Appl Environ Microbiol. 2002;68:1665–73.

74. Schultz B, Koprivnikar J. Free-living parasite infectious stages promote zooplankton abundance under the risk of predation. Oecologia. 2019;191:411–9.

75. Kaufman L, Rousseeuw PJ. Partitioning Around Medoids (Program PAM). In: Kaufman L, Rousseeuw PJ, (editors.) Finding Groups in Data: An Introduction to Cluster Analysis. Hoboken, NJ, USA: John Wiley & Sons, Inc.; 1990 [cited 2020 Mar 13]. p. 68–125. (Wiley Series in Probability and Statistics). Available from: http://doi.wiley.com/10.1002/9780470316801.

76. Ferrenberg S, O'neill SP, Knelman JE, Todd B, Duggan S, Bradley D, et al. Changes in assembly processes in soil bacterial communities following a wildfire disturbance. ISME J. 2013;7:1102–11.

77. Antunes J, Leão P, Vasconcelos V. Marine biofilms: diversity of communities and of chemical cues. Environ Microbiol Rep. 2019;11:287–305.

78. Stegen JC, Lin X, Konopka AE, Fredrickson JK. Stochastic and deterministic assembly processes in subsurface microbial communities. ISME J. 2012;6:1653–64.

79. Dantas LCDM, Da Silva-Neto JP, Dantas TS, Naves LZ, Das Neves FD, Da, et al. Bacterial adhesion and surface roughness for different clinical techniques for acrylic polymethyl methacrylate. Int J Dent. 2016;2016:8685796.

80. Eginton PJ, Gibson H, Holah J, Handley PS, Gilbert P. The influence of substratum properties on the attachment of bacterial cells. Colloids Surf B Biointerfaces. 1995;5:153–9.

81. Characklis WG, McFeters GA, Marshall KC. Physiological ecology in biofilm systems. In: Characklis GW, Marshall KC, (editors.) Biofilms. New York: John Wiley & Sons; 1990. p. 341–94.

82. Bredon M, Dittmer J, Noël C, Moumen B, Bouchon D. Lignocellulose degradation at the holobiont level: teamwork in a keystone soil invertebrate. Microbiome. 2018;6:1–19.

83. Langenheder S, Lindström ES, Tranvik LJ. Structure and function of bacterial communities emerging from different sources under identical conditions. Appl Environ Microbiol. 2006;72:212–20.

84. Caruso T, Chan Y, Lacap DC, Lau MCY, McKay CP, Pointing SB. Stochastic and deterministic processes interact in the assembly of desert microbial communities on a global scale. ISME J. 2011;5:1406–13.

85. Johansen R, Albright M, Gallegos-Graves LV, Lopez D, Runde A, Yoshida T, et al. Tracking replicate divergence in microbial community composition and function in experimental microcosms. Micro Ecol. 2019;78:1035–9.

86. Castle SC, Nemergut DR, Grandy AS, Leff JW, Graham EB, Hood E, et al. Biogeochemical drivers of microbial community convergence across actively retreating glaciers. Soil Biol Biochem. 2016;101:74–84.

87. Bik HM, Alexiev A, Aulakh SK, Bharadwaj L, Flanagan J, Haggerty JM, et al. Microbial community succession and nutrient cycling responses following perturbations of experimental saltwater aquaria. mSphere. 2019;4:e00043–19.

88. Tanaka M, Nakayama J. Development of the gut microbiota in infancy and its impact on health in later life. Allergol Int. 2017;66:515–22.

89. Pagaling E, Strathdee F, Spears BM, Cates ME, Allen RJ, Free A. Community history affects the predictability of microbial ecosystem development. ISME J. 2014;8:19–30.

90. Dawson FH, Kern-Hansen U. The effect of natural and artificial shade on the macrophytes of lowland streams and the use of shade as a management technique. Int Rev Hydrobiol. 1979;64:437–55.

91. Rittman BE. The effect of shear stress on biofilm loss rate. Biotechnol Bioeng. 1982;24:501–506.

92. Rochex A, Godon JJ, Bernet N, Escudié R. Role of shear stress on composition, diversity and dynamics of biofilm bacterial communities. Water Res. 2008;42:4915–22.

93. Holt RD, Lawton JH. The ecological consequences of shared natural enemies. Annu Rev Ecol Syst. 1994;25:495–520.

94. Schoener TW. & Spiller DA. Devastation prey diversity experimentally introduced predat field. Nature. 1996;381:691–4

95. Broglio E, Saiz E, Calbet A, Trepat I, Alcaraz M. Trophic impact and prey selection by crustacean zooplankton on the microbial communities of an oligotrophic coastal area (NW Mediterranean Sea). Aquat Micro Ecol. 2004;35:65–78.

96. Gómez F. Symbioses of Ciliates (Ciliophora) and Diatoms (Bacillariophyceae): taxonomy and host–symbiont interactions. Oceans. 2020;1:133–55.

97. Hessen DO, Elser JJ, Sterner RW, Urabe J. Ecological stoichiometry: an elementary approach using basic principles. Limnol Oceanogr. 2013;58:2219–36.

98. Ballantyne IVF, Menge DNL, Ostling A, Hosseini P. Nutrient recycling affects autotroph and ecosystem stoichiometry. Am Nat. 2008;171:511–23.

99. Mitra A, Flynn KJ. Predator-prey interactions: is "ecological stoichiometry" sufficient when good food goes bad? J Plankton Res. 2005;27:393–9.

100. Flynn KJ, Davidson K. Predator-prey interactions between Isochrysis galbana and Oxyrrhis marina. II. Release of non-protein amines and faeces during predation of Isochrysis. J Plankton Res. 1993;15:893–905.

101. Yang JW, Wu W, Chung CC, Chiang KP, Gong GC, Hsieh CH. Predator and prey biodiversity relationship and its consequences on marine ecosystem functioning - Interplay between nanoflagellates and bacterioplankton. ISME J. 2018;12:1532–42.